Department for communication and space technologies

Applied Optics Laboratory

Light pollution characterization module (LPCM) Hardware Design Document (HDD) Report 2022-03 (Funded by HRZZ and FERSAT)

Jakov Tutavac

June 29, 2022

Contents

1 Introduction

This document describes the design of the first light pollution characterization module (LPCM) prototype, which is an instrument intended to measure light pollution from Low-Earth Orbit (LEO) as a payload on a nanosatellite. The LPCM can also be used as a measuring tool on board a drone, baloon, or an aeroplane. The LPCM is a system uses detectors for detecting infrared, visible and ultraviolet light in specially defined spectral segments and used to categorize public illumination sources that appear on the surface of the Earth. The purpose of this document is to describe the details of the first build of the LCPM. The outline is given below:

- theoretical background
- hardware block diagram
- electrical schematics
- list of components
- technical drawings of 3-D printed enclosures

2 Instrument Overview

2.1 Block diagram

The instrument comprises custom designed electronic printed circuit boards (PCBs) and 3-D printed parts, and embedded algoritm to analyze data. The major parts are:

- s010x0 - main module PCB,
- s010x0_f01 - auxiliary adapter PCB,
- 3-D printed filter enclosure,
- 3-D printed adapter mount for installation on an integrating sphere.

The hardware block diagram is shown in Figure 1 and consists of several electronic components which together form a functional unit.

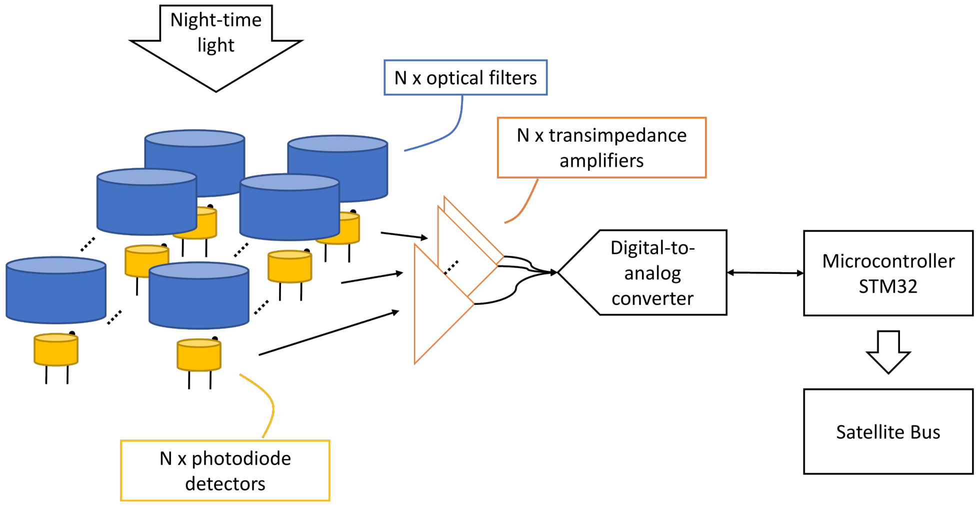

Figure 1: The hardware block diagram.

The instrument measures night-time light by optical detectors, which are light-sensitive consumer-off-the-shelf (COTS) components. The instrument has a set of photodiode detectors, which upon being illuminated generate a current in the range of nA (nano Amperes) or less. This photocurrent is amplified and converted into a voltage, ready to be digitized by an analog-to-digital converter. The measured data in digital format is acquired by a microcontroller which applies signal processing methods and formats the data for further use. The goal in capturing this data is to characterize the light source producing the observed light and will be detailed later in this document.

Each detector is paired with an optical filter, placed above the light-sensitive active area. Optical filters allow each detector to receive a different portion of the visible light to near-infrared spectrum, by filtering any incoming light. The transmission characteristics of the optical filters are shown in Figure 2. The reason behind the optical filters will, again, be detailed later in this document.

2.2 Brief hardware description

The main part of the instrument hardware is the main module PCB, for which the front side and the back side are shown in Figures 3a and 3b, respectively. A channel of the

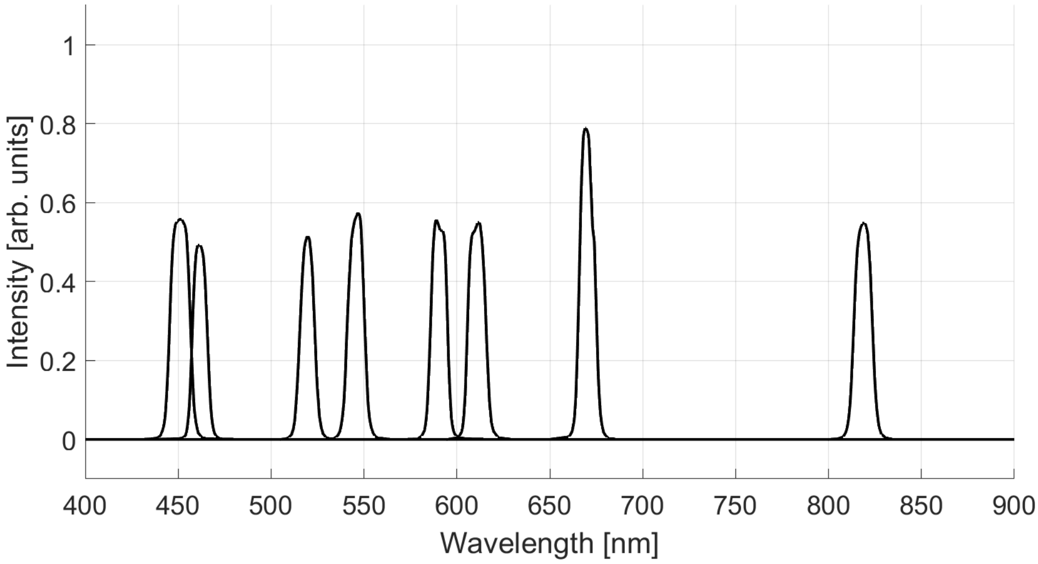

Figure 2: The filtering characteristic of the optical filters.

instrument denotes the triplet consisting of an optical filter, a detector, and an amplifier. The detectors are visible on the front of the board, Figure 3a. The amplifiers are visible on the back of the board, Figure 3b, with traces routed from each amplifier to the analog-to-digital converter. The optical filters are not shown in the two above-mentioned figures.

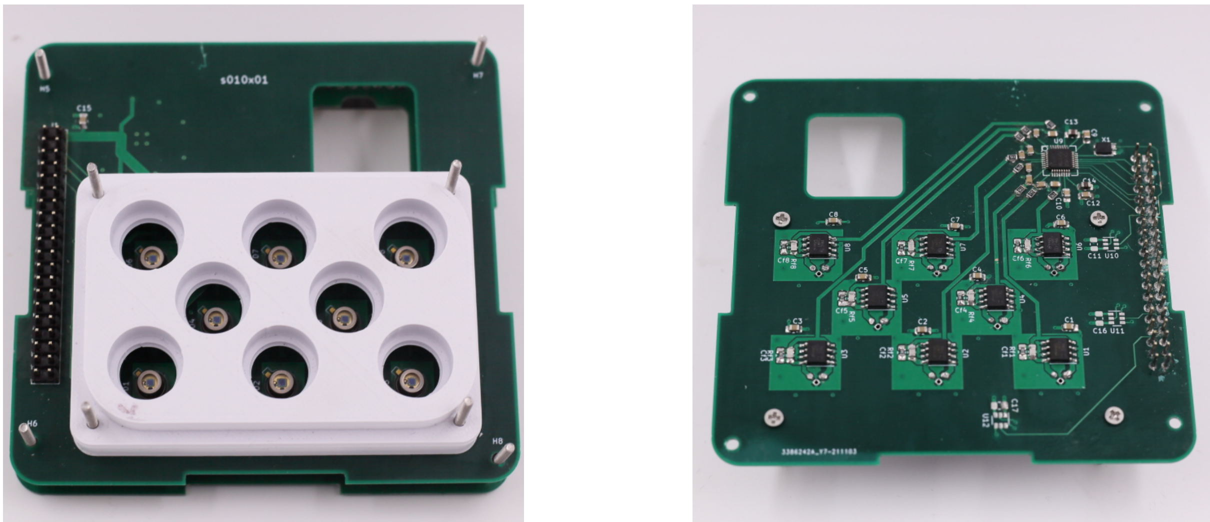

(a) Front side with filter enclosure.

(b) Back side.

The output of each channel is a positive voltage value, which is proportional to the intensity of filtered light impinging the detector. The output value is different for each channel, since the optical filters differ, which means the device produces spectrally resolved (in wavelength) measurement data. This is important because such data allows identification of the type of source from the measured light.

The optical filters must be placed above the detectors to filter the light, which is why a custom 3-D printed enclosure is used, as is shown in Figure 3a. When a filter is placed inside the enclosure hole opening of a channel, only light passing through the filter reaches the light sensitive part of the detector. The filters are held in place by a custom designed metallic board, which is shown in Figure 4a. This simple setup is convenient for testing purposes as replacement of filters requires only removing screws and bolts.

The instrument includes an integrating sphere mount adapter, shown in Figure 4b, which allows installation onto an integrating sphere to simplify measurements. An example is shown in Figure 5, where the instrument is placed on an integrating sphere and a discharge lamp is the measured light source. When the instrument is placed in-front of a light source, the light travels in a straight path from the source to the detectors. Since the light source radiates in many directions, not all detectors observe the source at the same spatial position and from the same angle. This results in an uneven amount of light reaching each detector, where in an extreme case one detector might be saturated with light and one detector might not sense any light. An integrating sphere is used to equally distribute the light on each detector.

A microcontroller is a necessary component of the instrument to control the analog-to-digital converter and provide a user-friendly way to measure target light sources. Development boards provided by microcontroller manufacturers ease development of hardware. The STM32F4 Discovery Board, which is shown in Figure 4c, features a powerful ARM Cortex-M4 32-bit microcontroller with IEEE754-compliant single-precision floating-point computation, as well as a range of native hardware instructions for multiplication and arithmetic.

The second PCB is the auxiliary adapter, shown in Figure 4d, which allows to connect a microcontroller with the analog-to-digital converter. The adapter fits onto an STM32F4 Discovery development board, shown in Figure 4c, which has an STM32 microcontroller ready for programming and transfer of measurement data.

Power to the main module is delivered through the adapter as well as electrical signals necessary for data transfer and control. Measurement data are, therefore, sent from the main module, through the auxiliary adapter, and are received by the STM32 microcontroller. In-house developed code, which runs on the microcontroller, provides the necessary functionality to operate the instrument and acquire measurements of desired target light sources.

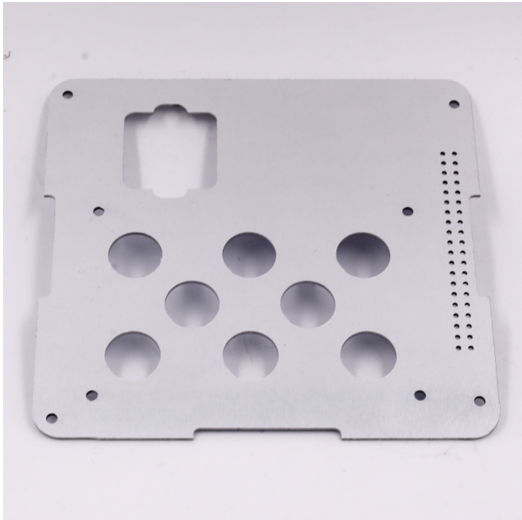

(a) Front filter holder.

(b) Integrating sphere mount.

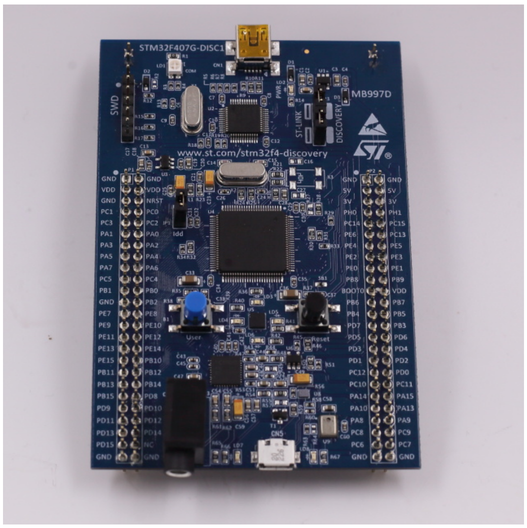

(c) STM32F4 Discovery board

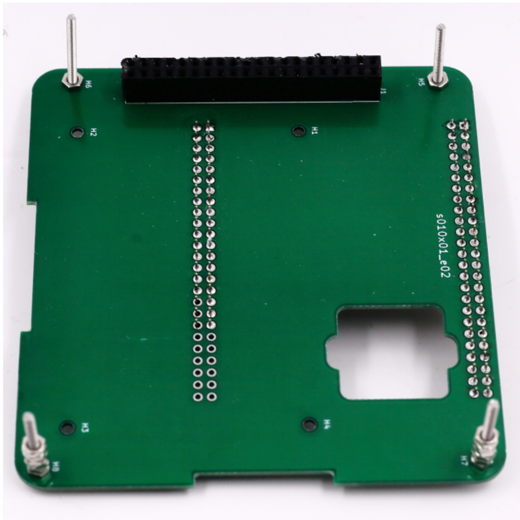

(d) Adapter for the STM32F4 board.

Figure 4: Instrument hardware.

Figure 5: Installation of the module onto an integrating sphere. A discharge lamp placed near the entrance port of the sphere produces light which travels inside the sphere and reflects onto each detector of the instrument. At the top of the sphere is an entry port for coupling the same light into a spectrometer fiber input.

3 Hardware design

3.1 Theory of operation

The LPCM instrument measures night light produced by public illumination sources. It is unclear what measuring light means and we provide our own definition here. By measuring light, we mean that the instrument observes light during a finite time interval and discovers the characteristics of the light source(s) producing this light, where of interest are: the type of light source and the strength of light produced by each source. By strength of light, we mean the fractional intensity of the total power of the light emitted by each source which contribute to the total captured optical power.

Next, we describe how the instrument measures light sources. Placing a single light source in an enclosed box or a dark room and observing the light produced from this source by the instrument results in characteristic measurement data. The identification of this light source is trivial, as we know that the shape of the spectrally resolved measured data corresponds to this source. This example can be generalized to any light source and is defined to be a calibration procedure for which light sources the instrument is calibrated. A set of reference data is constructed by the calibration procedure as it is repeated to many different light sources.

The instrument determines the characteristics of the sources for any other case, when two or more light sources are present. The most natural example is the case of measuring a light source with background sunlight. The observed data are compared with all reference data constructed by the calibration procedure. When matching data is found in the reference data, both of the sources can be identified and the strength of each source in the light mixture can be determined.

So far we showed how spectrally resolved data can be used for identification of the type of source. However, we stopped short at detailing the optical filters. We address the following questions: (1) What are the characteristics of the optical filters and (2) What is the sufficient number of filters sufficient to characterize the public illumination soruces with high accuracy.

Filter characteristics The shape of the resolved data is due to optical bandpass filters, which reject light that is outside a narrow wavelength region specified by two values: the central wavelength (CWL) and the full-width at half-max (FWHM). Table 1 includes a list of the optical bandpass filters used. To answer why these filters are used, we must understand the nature of the technology for artificial lighting. A short summary is given, while the details can be found in literature.

The light sources typically used for public lighting include: white LEDs, high-pressure sodium, high-pressure mercury, and metal-halide lamps. These light sources are used for public lighting due to their advantageous technical properties (energy efficacy and color rendition) and due to imposed governmental regulations on efficacy and light power emission. There are three major differences between the spectra of white LEDs and discharge lamps. White LEDs (*i*) emit broadband light, (*ii*) produce substantial blue light emission, and (*iii*) produce no emission in the wavelength regions above of red light. All of the three characteristics are due to the differences in the physical phenomena and technology behind the white LEDs and discharge lamps.

While solid state lighting is based on a semiconductor junction producing light, discharge lamps depend on plasma gas to radiate light. The light emitted by discharge lamps dramatically varies depending upon the plasma composition, or in other words, upon the constituent atomic elements. Therefore, the spectra of discharge lamps consist of numer-

Filter code	CWL [nm]	FWHM [nm]
	310	10
	320	10
450DIB12	450	10
460DIB12	460	10
520DIB12	520	10
546DIB12	546.1	10
589DIN12	589.6	3

Filter code	CWL [nm]	FWHM [nm]
610DIB12	610	10
670DIB12	670	10
820DIB12	820	10
1020DIB12	1020	15
1140DIB12	1140	17.5
1300DIB12	1300	12

Table 1: List of bandpass filter components purchased. Specified with central wavelength (CWL) and full-width at half-max (FWHM) values in nm.

ous spectral emission lines which emerge by spontaneous emission of photons from the plasma gas. The significant atomic elements contained within the plasma gas may include: sodium, mercury, and metals such as indium, thallium and lithium. The principal spectral emission lines are found in reference books or online [1], a part of which was used to construct Table 2. The table lists spectral lines with ascending wavelength, denoting the atomic element and the light source(s) where the emission line is present. The light source types are denoted as HPS, HPM, and MH; which is short for high-pressure sodium, high-pressure mercury, and metal halide, respectively.

Atomic element	Spectral line [nm]	Light sources presence
Hg	365.0	HPM, MH
Hg	404.7	HPM, MH
Hg	435.8	HPM, MH
In	450	MH
Na	497.8/498.3	HPS
Tl	534	MH
Hg	546.1	HPM, MH

Atomic element	Spectral line [nm]	Light sources presence
Na	568.3/568.8	HPS
Hg	577.0	HPM, MH
Hg	579.1	HPM, MH
Na	589.0/589.6	MH
Li	610	MH
Na	615.4/616.1	HPS, MH
Li	670	MH
Na	818.4/819.5	HPS, MH

Table 2: Spectral lines of atomic elements commonly present in discharge lamps for the wavelength region from 350 nm to 850 nm. Data is taken from [1].

Given the two tables, one for the characteristics of the filters, and one for the spectral emission lines of the atomic elements which cause the emission, one might ask are the entries in the tables related. The answer is yes, the specifications of the filters are correlated with the spectral emission lines of the atomic elements. In fact, the filters are chosen as to maximize the orthogonality of the spectra.

Measured spectra can be linearly combined into a mixture spectrum. The spectra therefore form a basis. When the spectra are orthogonal the inverse process, where from a mixture spectrum we determine the coefficients of the linear combinations, can be solved uniquely. While it is desired that the spectra are orthogonal, such that they do not overlap at any filter, in practice this is not possible. However, by choice in filters the spectra can be made partially orthogonal. The closer the measured spectra by the instrument are to orthogonal spectra, the better the estimated inverse result will be and the characteristics of the source are estimated more accurately.

Let us explain what we mean by partially orthogonal spectra. Let all filters be non-overlapping in their transmission characteristic. Let us denote a spectrum as one spectrum of all the spectra of light source types taken in consideration, such as the ones mentioned in the preceding paragraphs. By partial orthogonality, we mean to find a set of optical bandpass filters, such that:

Before we address the second question, regarding the number of filters, we must note the effect the temporally resolved data has on identification of source types.

The number of filters is tied intimately with the number of types of light sources which we can differentiate. The more filters, the more types we can resolve. But in practice, the constraints in size, weight and volume of the instrument limit the number of filters and conversely limit the number of categories of light sources.

In conclusion, the number of channels (filters) is a design constraint by the size and volume constraints of the instrument and is fixed to be eight. The characteristics of the filters listed in Table 1 are correlated with the spectral emission lines listed in Table 2, and are chosen as to optimize identification of different types of desired light sources.

3.2 Design as a payload

The CubeSat format is a standard describing a set of rules for designing small satellites. The format is popular for its lowered entry costs to launch a payload into orbit. The base constraints for the 1-U (one unit) are: 10 cm $\times$ 10 cm $\times$ 10 cm, and approximately 1 kg of mass. Larger CubeSat formats are available such as 2-U, 3-U, 6-U, and even 12-U.

It is challenging to design payloads for the CubeSat format due to tight space, volume and weight constraints. In addition, there are limits in available power which are prohibitive for on-board data processing. In specific, the payload design is limited to a single PCB, with four mounting holes for attaching the board onto the satellite frame and one connector for inter-board connections.

One of the problems met while designing the main PCB was regarding the mechanical board outline, which is shown in Figure 6. More specifically, the outline does not align well with the default grids available in the CAD software. This causes problems when trying to draw dimensions on the board. In addition, placing parts such as mounting holes and connectors with respect to the board outline showed to be difficult. To place such a component, additional user drawn lines on a separate layer were required to draw vertical and horizontal grid lines extended from the outline to the desired location. It is important that the mechanical board outlines follow one of the grid settings available in the CAD software used.

One problem met after assembling the main PCB was regarding the thickness of the board, which is 0.8 mm. The main connector is used to install the main PCB with the adapter PCB. It is difficult to remove one PCB from another, once they have been connected together. Careful removal is required in order not to apply too much force on the board since it can bend and brake. For future revisions, it is important to use a board thickness of at least 1 mm.

3.3 Optical filters

Detailed requirements on the characteristics of the filters are listed in in Table 1. Optical bandpass filters are commonly available as consumer off-the-shelf components (COTS),

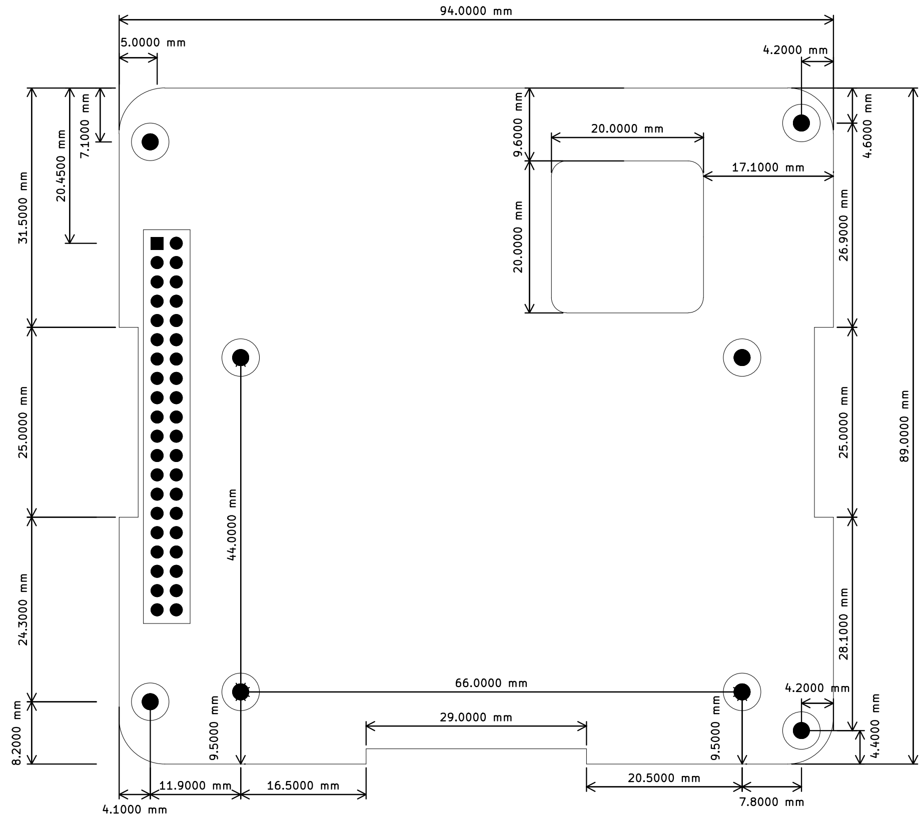

Figure 6: Board outline with annotated dimensions.

with central wavelength (CWL) values from UV to near-infared light and full-width at half-max (FWHM) values from 5 nm, 10 nm, 25 nm, to up to 50 nm. Since the bandpass filters must cover the active area of the detector, their size is one of the limiting factor when deciding on the number of channels. COTS bandpass filters are commonly available at sizes ranging from 1.27 mm (0.5 inch) to 2.54 mm (1 inch). Custom made optical bandpass filters can be designed for specific required CWL and FWHM values and sizes, however their high cost and design time is prohibitive for prototypes.

Each optical bandpass filter produces light at its output which is of intensity at least one order of magnitude less, when compared to the input light. The amount of light rejected is very wavelength dependent and is denoted as insertion loss and can be expressed in units of dB. The insertion loss of the filters acquired is between 1 dB and 3 dB at the peak wavelength in the passband region.

3.4 Optical detectors

The following text describes the function and the exact specifications of the optical detectors used. The instrument uses a set of photodiode detectors, which generate a photocurrent proportional to the impinging light, to measure and characterize light sources.

Photodiodes are abundantly available as consumer off the shelf components and the packaging technology can be surface mount or through hole. The ideal design would use detectors which all have the same package, such that no adjustments have to be made regarding placement of the detectors with respect to the optical filters. For that reason, we placed a design requirement for all detectors to be fitted into a transistor outline (TO) package family. TO is a type of metal can which is hermetically sealed to protect the device from environmental factors such as moisture and contaminants. Photodiodes are most commonly packaged as (in increasing size): TO-18, TO-5, and TO-8.

With the intent of minimizing the size and weight of the detectors the TO-18 package was chosen. The package dimensions are: diameter 5.6 mm, height 3.8 mm, through hole pin spacing 2.54 mm, through hole pin diameter 0.45 mm. However, using a TO-18 packaged photodiode is not optimal and the reason is that the optical elements are larger in diameter, 1.27 mm when compared to 5.6 mm.

The chosen silicon detectors are S2386-18K manufactured by Hamamatsu. The detectors are in a TO-18 package. The specifications of the detectors are listed next. The active area is a square with dimensions of 1.1 $\times$ 1.1 mm and area of 1.21 mm^2. The The rated operating temperature is from $-40\,^{\circ}\mathrm{C}$ to $100\,^{\circ}\mathrm{C}$. The sensitivity peaks at 960 nm with a value of $0.6\,\mathrm{A\,W^{-1}}$. Noise equivalent power at 960 nm is $6.8 \cdot 10^{-16}$ $\mathrm{W/Hz^{1/2}}$. The stated dark current is 100 fA at 10 mV of reverse voltage applied. The directivity at an angle of 45 degrees from the center is 50 percent.

There are two issues with the chosen detectors which should be considered for future revisions. First is the package size where larger TO-5 or TO-8 detectors are to be considered. Second is that the window material is borosilicate glass, which is not suitable for a space environment due to solarization affecting the transmission properties of the glass. Instead, detectors which use a quartz window material must be used.

3.5 Amplifier

The following text describes the function and the exact specifications of the amplifier used. Photodiode detectors generate a photo-current proportional to the impinging light in the order of a few nA, which is difficult to measure. A transimpedance amplifier can be used to convert the faint photo-current into a much larger voltage.

The LMP7721 is a precision CMOS amplifier, manufactured by Texas Instruments and offered in an 8-pin SOIC package. The base preamplifier circuit includes the LMP7721, connected with the negative input to the kathode of the photodiode detector and connected with the positive input to the ground. The negative feedback consists of a resistor R_f and a parallel capacitor C_f.

The amplifier gain is determined by the value of the feedback resistor and is frequency dependent. The response is flat until either the feedback capacitor or either the closed loop gain of the amplifier degrade the characteristic. The gain bandwidth product of the LMP7721 is 17 MHz.

The specifications of the LMP7721 are listed next. The stated input bias current is limited within ± 20 fA at $25\,^{\circ}\mathrm{C}$. The required voltage supply is in range of 2 V to 5.5 V, but the maximum voltage supply difference between the positive and negative supply is 6 V. The rated operating temperature is from $-40\,^{\circ}\mathrm{C}$ to $125\,^{\circ}\mathrm{C}$. The typical offset voltage is ± 26 µV with a typical drift of $-1.5\,\mu\mathrm{V\,^{\circ}C^{-1}}$.

3.6 Analog-to-digital converter

The following text describes the function and the exact specifications of the analog-to-digital converter (ADC) used. The voltage at the output of the transimpedance amplifier is converted into a digital value by the ADC.

The device chosen is the ADS131M08, manufactured by Texas Instrument. It is a complex ADC which is offered in a 32-pin TQFP (5 $\times$ 5 mm) or a leadless 32-pin WQFN

(4 × 4 mm) package, enabling operation from −40 °C to 125 °C.

This device was chosen due to its eight simultaneously sampling channels, where each channel is sampled by its own delta-sigma ADC. Each channel includes an optional programmable gain amplifier. The device includes a 1.2 V reference integrated which reduces the required printed circuit board area. The only required external component is the clock source, such as the 8.096 MHz clock integrated circuit DSC1001CI2-00B.1920T.

The input impedance of the ADC depends on the gain of the in-built PGA. For low gain values $[1, 2, 4]$, the input impedance is 330 kΩ. For higher gain values $[8, 16, 32, 64, 128]$, the input impedance is approximately 2 MΩ. These values are valid only when the device is working in the high-resolution mode.

The ADS131M08 features an internal analog test signal that is useful for troubleshooting and diagnosis. A positive or negative DC test signal can be applied to the channel inputs through the input multiplexer. The test signal is shared by all channels, and is internally generated as $2 \cdot V_{ref}/15$, where $V_{ref} = 1.2$ V.

Captured data is transmitted serially, and the serial clock rate is limited by the external clock ($f_c = 8$ MHz). One of the problems with increasing the serial clock is the increase of digital noise in the board. Yet another problem with increasing the serial clock rate is the signal integrity of the digital outputs sent from the ADC to be received by the microcontroller. A fast clock might cause communication errors and faulty readings. The ADC captures the data for eight channels simultaneously and transmits this data in as 10 words, where each word by default has 3 bytes of data, resulting in a frame with $10 \cdot 3 \cdot 8 = 240$ bits. The serial bitrate of the STM32 microcontroller is programmed to be 2.625 Mbps. The time required for one frame to be transferred is $T_f = 240/2.625 = 91.43$ µs. The sampling rate of the ADC depends upon the external clock rate, denoted by f_c, and a programmable oversampling ratio, denoted by OSR, as $f_s = f_c/(2 \cdot OSR)$. For $f_c = 8.192$ MHz and $OSR = 8192$, the sample rate is $f_s = 500$ Hz and the sampling period is $T_s = 1/f_s = 2$ ms. The frame transfer time is much smaller than the sampling period: $T_f \ll T_s$. This is true when the sampling rate is doubled. It is even true for the case when the sampling rate is doubled and the serial bitrate is halved.

References

[1] Handbook of Basic Atomic Spectroscopic Data. NIST Standard Reference Database 108. 2013. doi:10.18434/T4FW23

4 Technical drawings

List of Figures

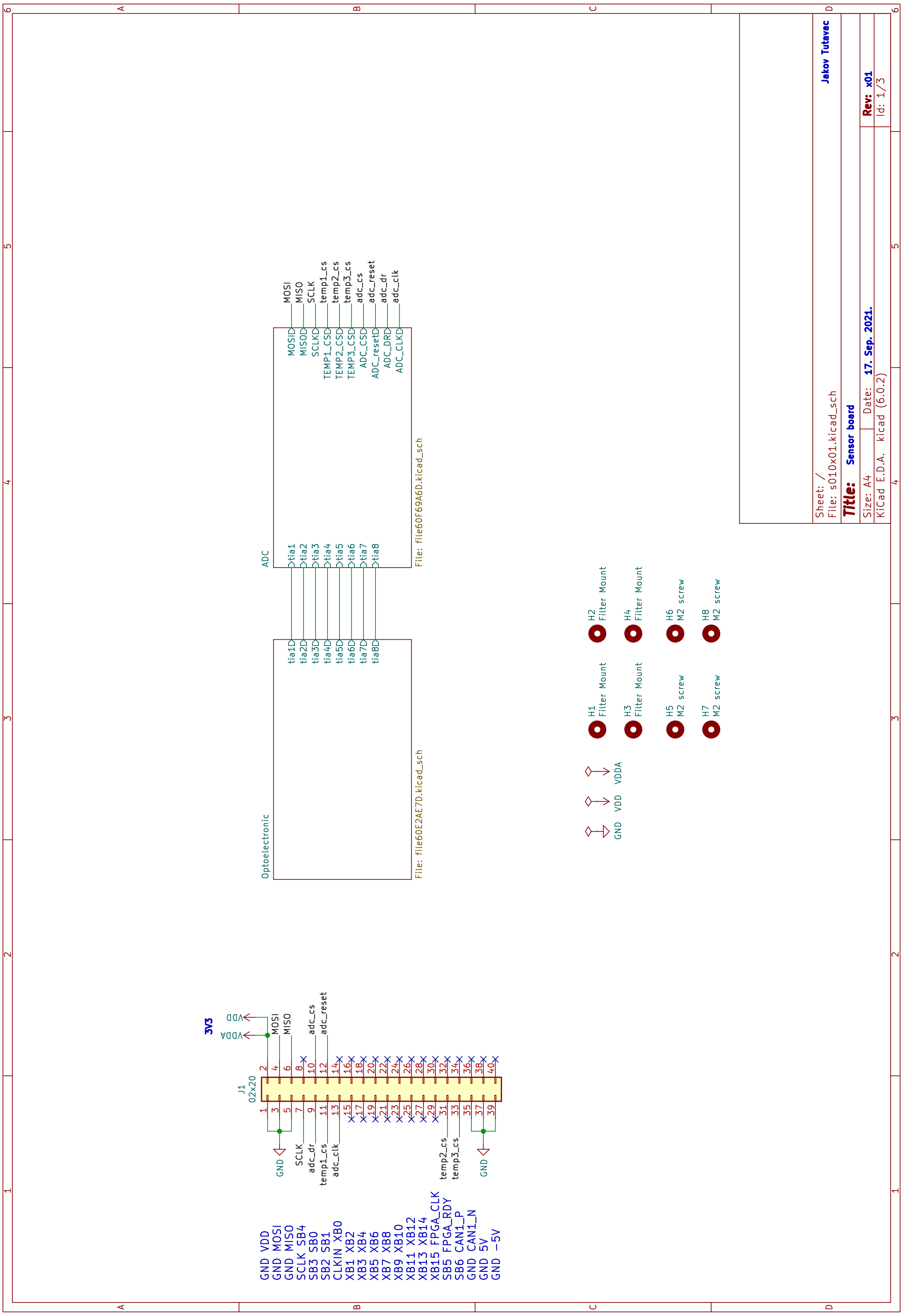

Figure 7: Electrical schematic: s010x0.

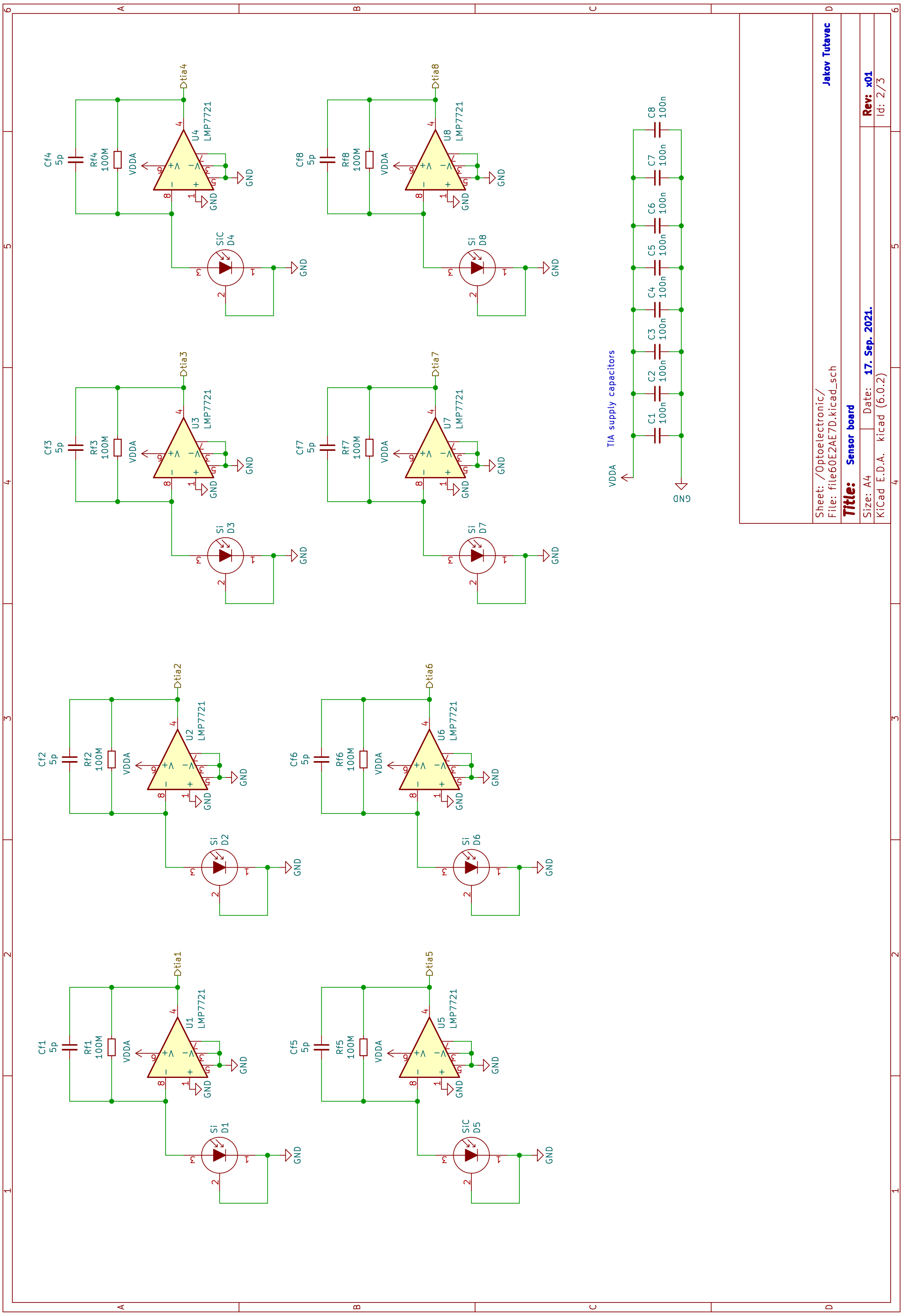

Figure 8: Electrical schematic: s010x0. Cont.

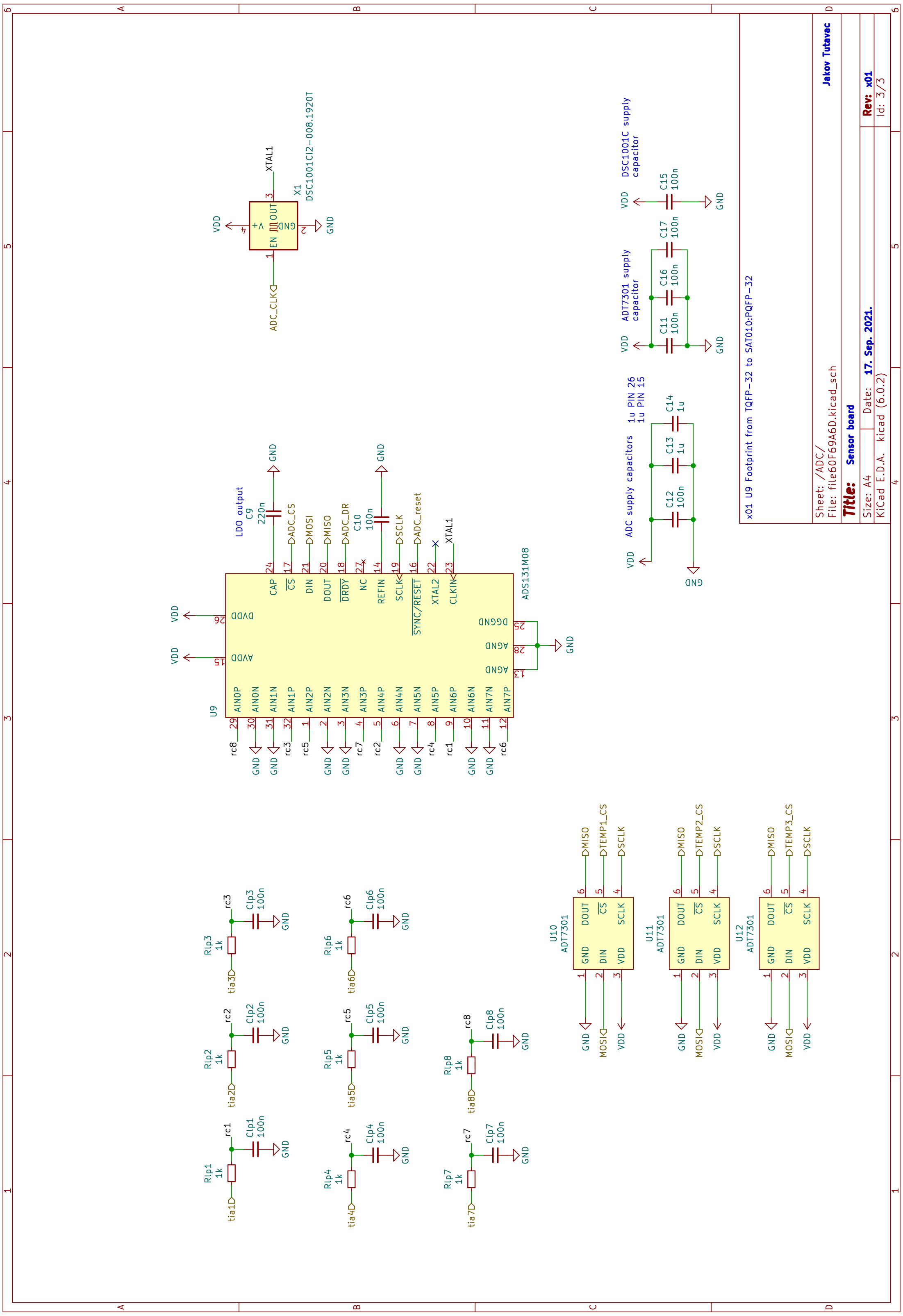

Figure 9: Electrical schematic: s010x0. Cont 2.

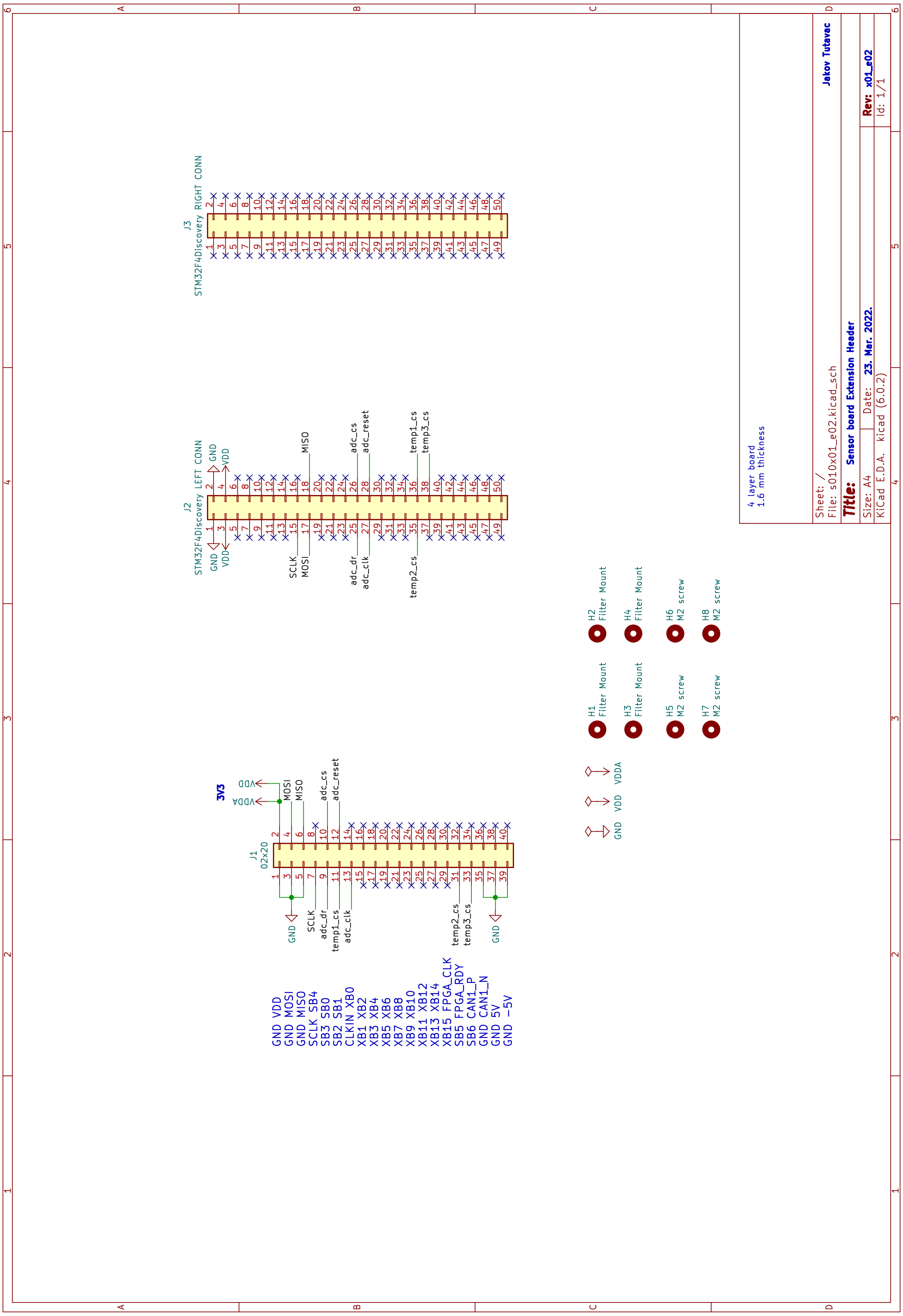

Figure 10: Electrical schematic: s010x01_e02.

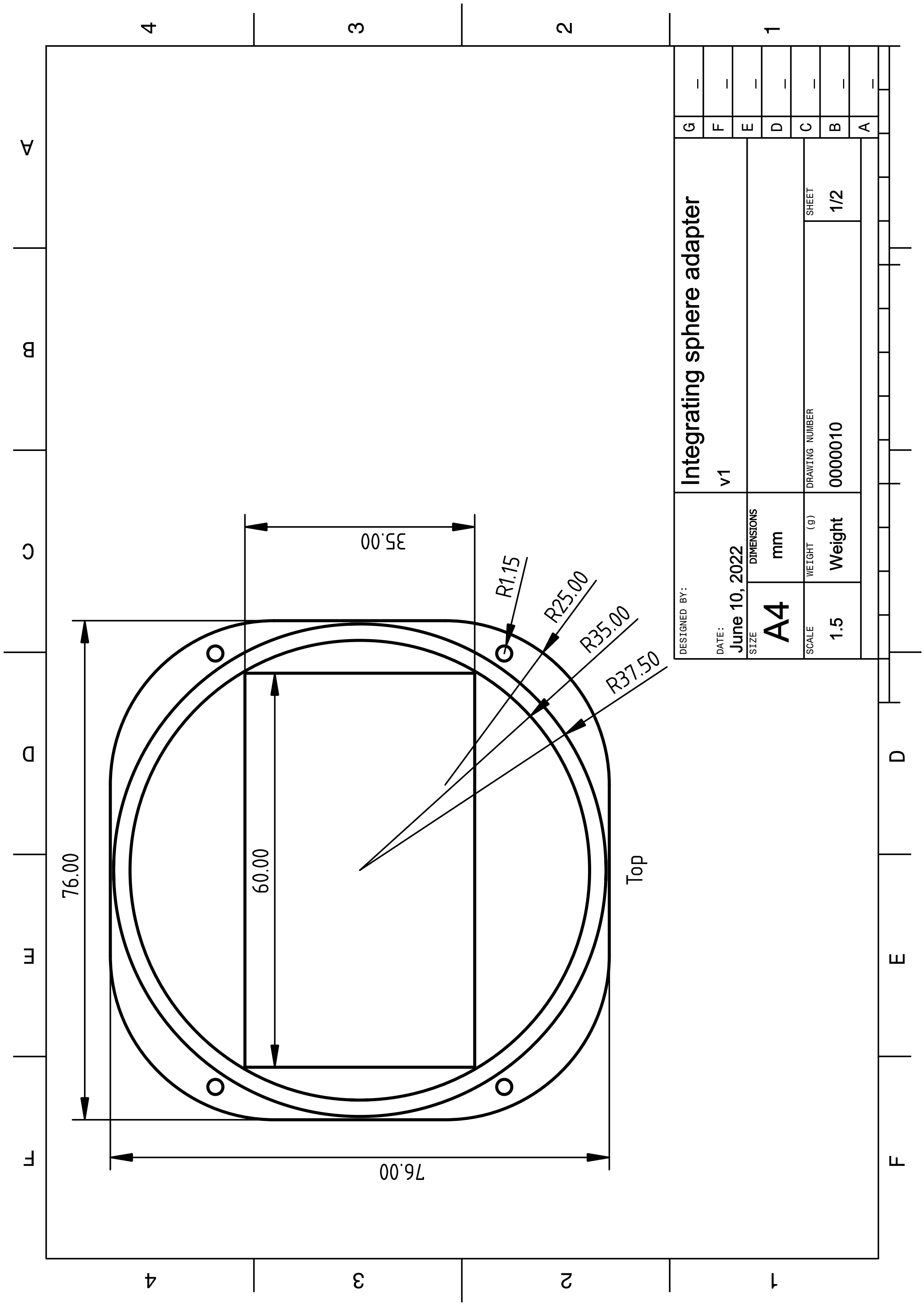

Figure 11: Drawing: Integrating sphere adapter. Top View.

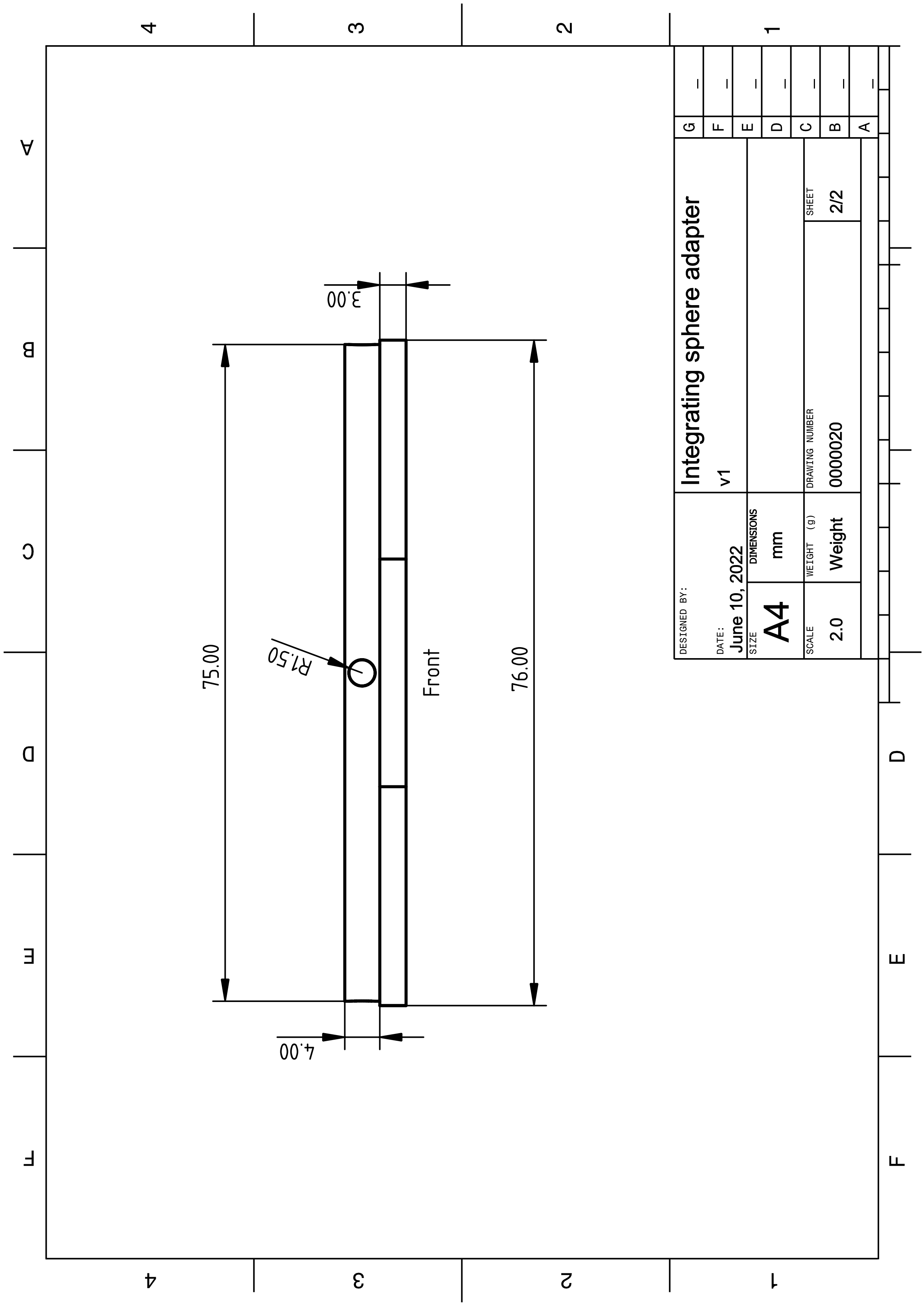

Figure 12: Drawing: Integrating sphere adapter. Front View.

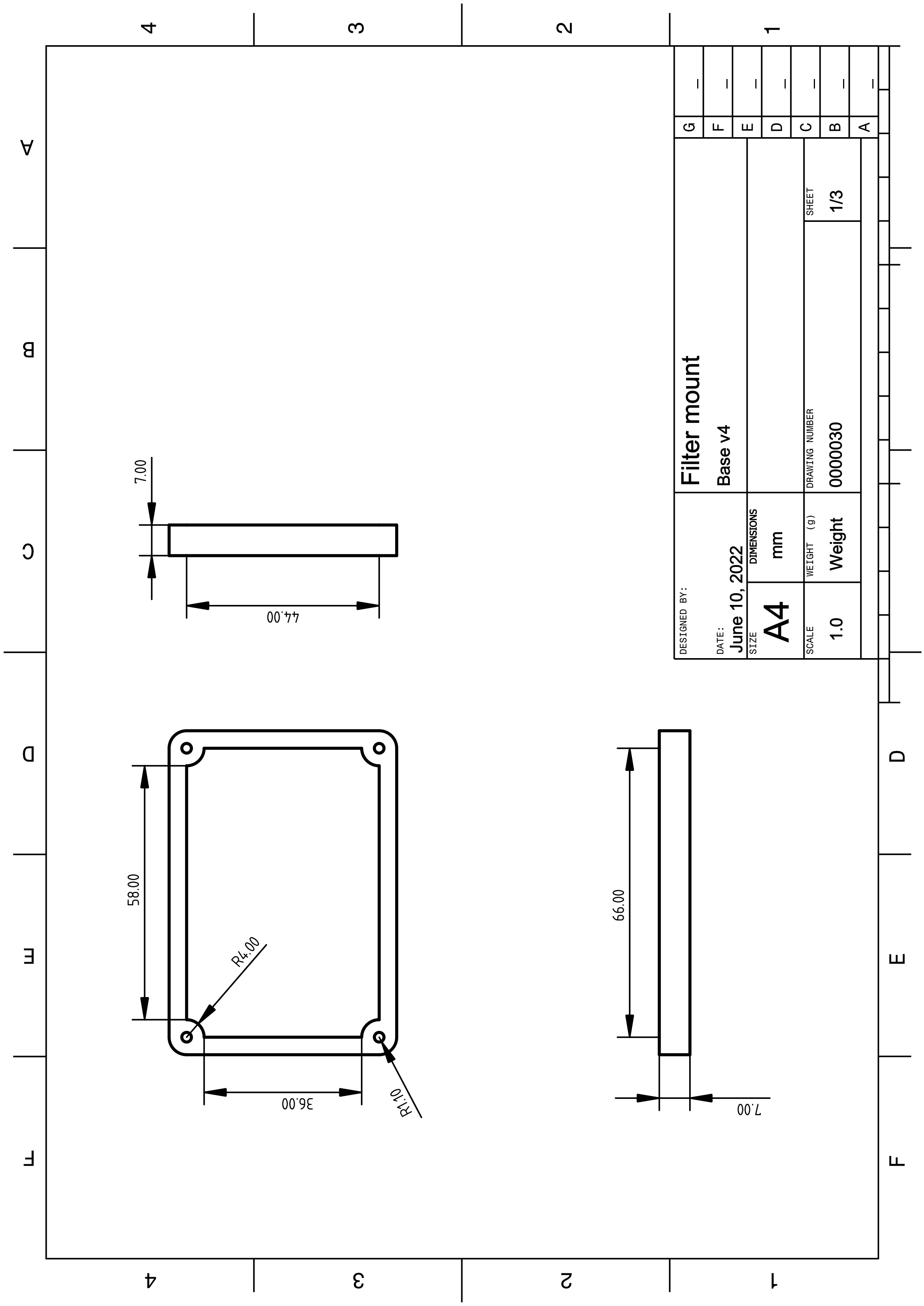

Figure 13: Drawing: Filter mount. Base.

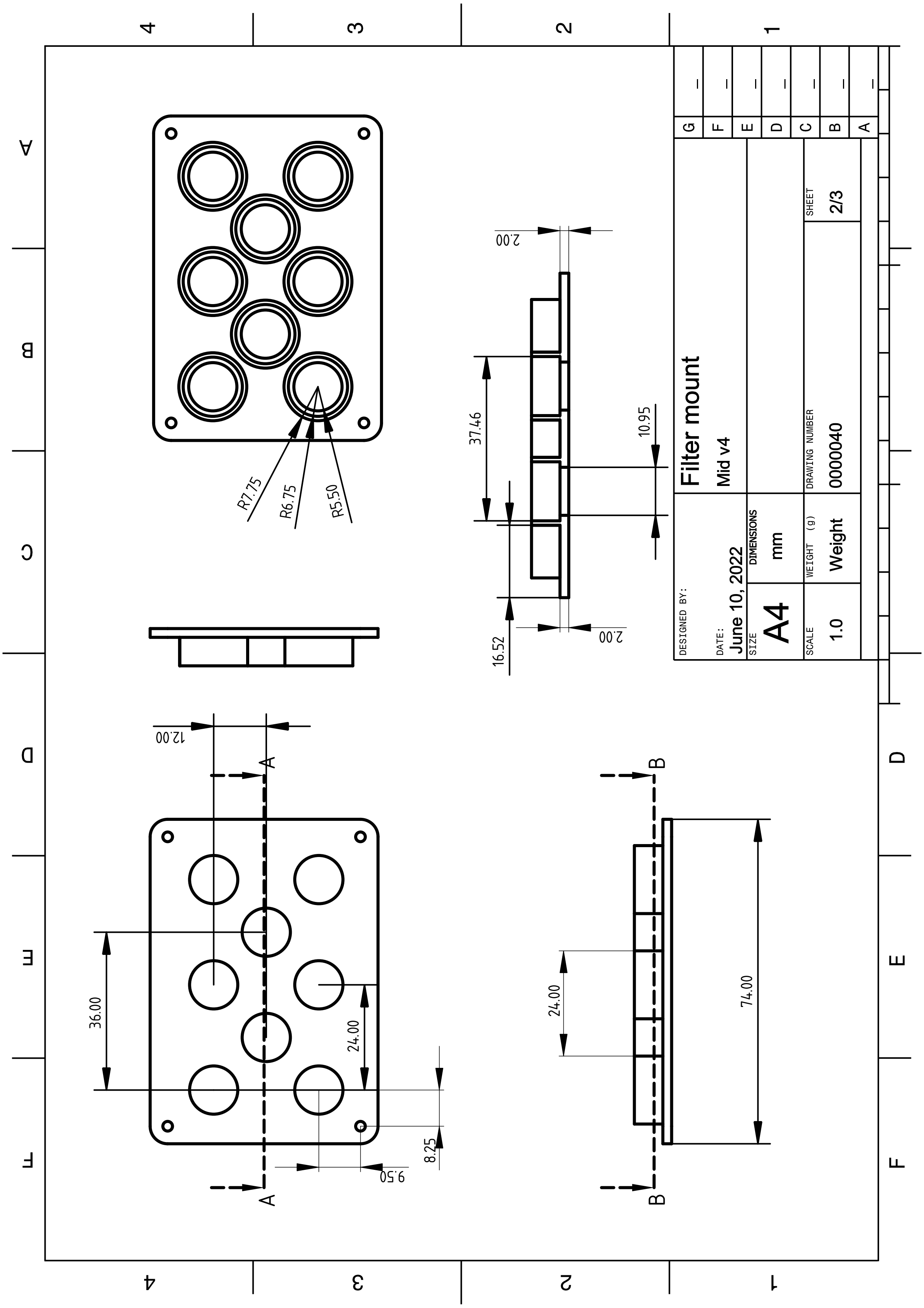

Figure 14: Drawing: Filter mount. Mid.

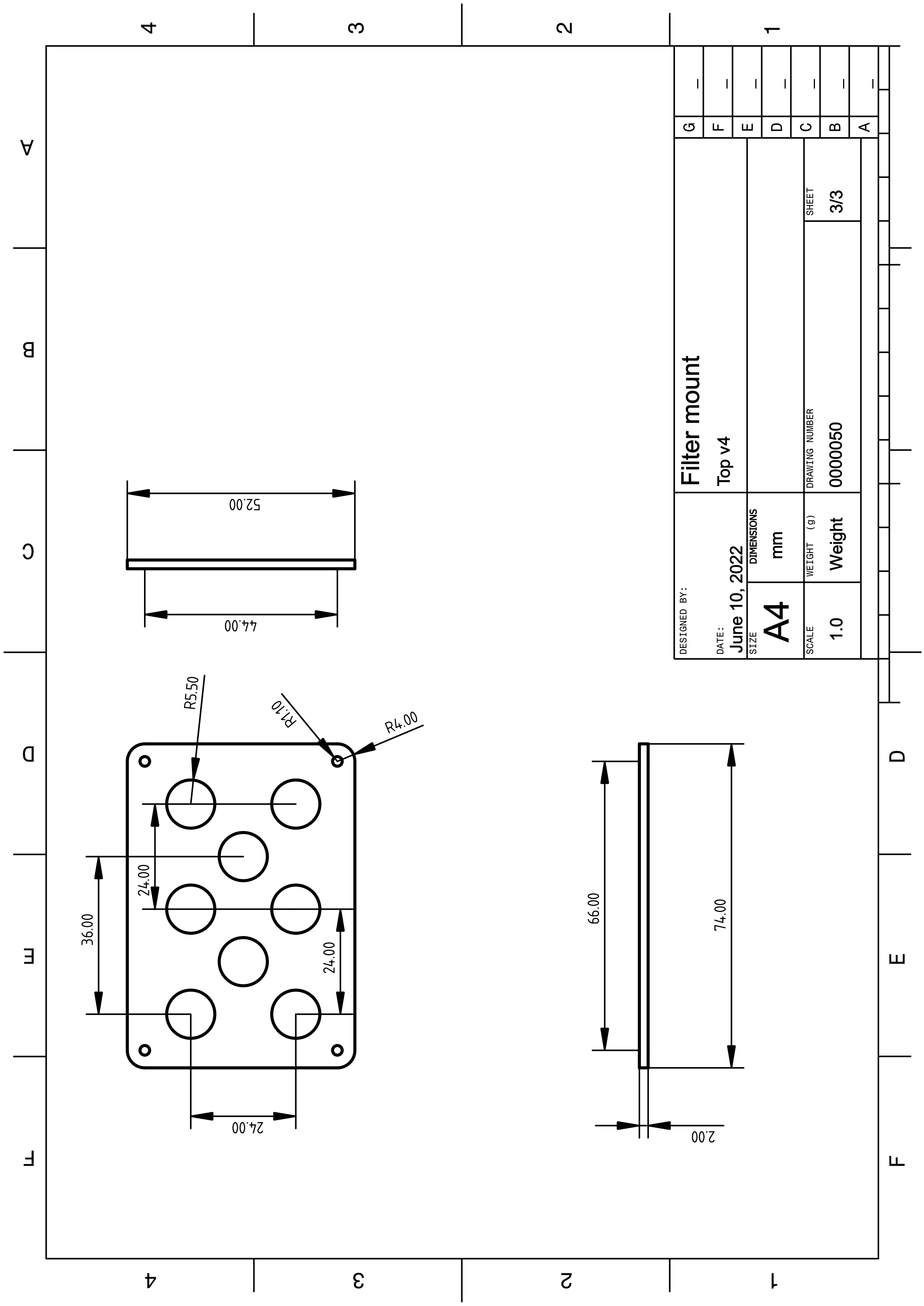

Figure 15: Drawing: Filter mount. Top.